

Ant Colony Optimization Approach To THD Analysis in Multilevel Inverter with Different Levels

Adeyemo, I. A.¹, Fakolujo, O. A.², Adepoju, G. A.³

Dept. of Electronic & Electrical Engineering,³Ladoke Akintola University of Technology, PMB 4000, Ogbomoso, Oyo State, Nigeria^{1,3}

Dept. of Electrical & Electronic Engineering, University of Ibadan, Ibadan, Oyo State, Nigeria²

ABSTRACT: In this paper, Variable Sampling Ant Colony optimization (SamACO) algorithm with random initial values is applied to Selective Harmonic Elimination (SHE) equations of 7-, 11-, and 15-level inverters in order to investigate the effects of increasing number of levels on the harmonic profile of the inverters. Solutions sets and their corresponding Total Harmonic Distortion (THD) are computed for each of the multilevel inverter structures at different modulation indices. Performance evaluation of the three multilevel inverter structures show that both 7-level and 11-level inverters are at par in terms of range of solution sets while 15-level inverter has a narrower range. Both 11-level and 15-level inverters have better harmonic profile compared with 7-level inverter for all values of modulation index. However, at some modulation indices, 11-level inverter has better harmonic spectrum compared with 15-level inverter, which shows that with evolutionary algorithm, increase in number of levels does not guarantee total elimination of the selected harmonics or lower THD for all values of modulation indices. Computational results are validated with MATLAB simulations.

KEYWORDS: Multilevel inverter, SamACO, selective harmonic elimination (SHE), evolutionary algorithms, THD.

I. INTRODUCTION

The advent of fast switching semiconductor devices has enabled the construction of relatively high power converters with improved harmonic spectrum using relatively low power semiconductor devices. The concept of utilizing multiple small voltage steps to perform power conversion originated from the idea of step approximation of sinusoid [1]. The smaller voltage steps yield lower switching losses, improved power quality, lower electro-magnetic interference (EMI), and lower voltage change rate (dv/dt). As the number of levels increases, the synthesized output waveform adds more steps, producing a staircase waveform with harmonic distortion that tends towards zero. However, the number of semiconductor switches increases with the increasing number of levels. Each semiconductor switch added requires associated gate drive circuitry. Hence, the cost as well as switching losses will increase and the circuit becomes complex [2]. The choice of number of levels in a multilevel converter is a tradeoff between cost, efficiency, complexity and THD.

Harmonic elimination in multilevel converters has been the focus of intensive research for many decades. To improve converters performance and output power quality, several modulation techniques used in conventional two-level inverter have been modified and deployed in multilevel inverters. These include Sinusoidal Pulse Width Modulation (SPWM), Selective Harmonic Elimination (SHE) method, Space Vector Control (SVC), and Space Vector Pulse Width Modulation (SVPWM) [3]. Selective Harmonics Elimination (SHE) method at fundamental switching frequency however, arguably gives the best result because of its high spectral performance and considerably reduced switching loss. Selective Harmonic Elimination (SHE) or programmed pulse width modulation scheme is a switching

International Journal of Innovative Research in Science, Engineering and Technology

(An ISO 3297: 2007 Certified Organization)

Vol. 4, Issue 9, September 2015

technique for inverters that provides direct control over the output waveform harmonics. In this method, the switching angles are chosen (programmed) to eliminate selected harmonics while the fundamental harmonic is satisfied. The implementation of this technique involves solving S number of equations in order to eliminate $(S-1)$ selected low order harmonics. With the increasing number of equations, the inverter voltage waveform approaches a nearly sinusoidal waveform with low harmonic distortion. However, the major drawback of this approach is the heavy computational burden involved in solving the transcendental nonlinear equations known as SHE equations that characterize the harmonics.

Several methods that have been reported for solving SHE equations can be classified into two groups: The first group is based on deterministic approach using exact algorithms. Newton Raphson iterative method [4] is one of these. The main disadvantage of iterative methods is that they diverge if the arbitrarily chosen initial values are not sufficiently close to the roots. They also risk being trapped at local optima and fail to give all the possible solution sets. Chiasson *et al* [5] proposed a method based on Elimination theory using resultants of polynomials to determine the solutions of the SHE equations. A difficulty with this approach is that as the number of levels increases, the order of the polynomials becomes very high, thereby making the computations of solutions of these polynomial equations very complex. Another approach uses Walsh functions [6], [7], [8] where solving linear equations, instead of non-linear transcendental equations, optimizes the switching angle. The method results in a set of algebraic matrix equations and the calculation of the optimal switching angles is a complex and time-consuming operation.

The second group is based on probabilistic approach using evolutionary algorithms that minimize rather than eliminate the selected harmonics. Evolutionary algorithms such as genetic algorithm [9], [10], [11], particle swarm optimization [12], ant colony system [13], bee algorithm [14] etc are derivative free and are successful in locating the optimal solution, but they are usually slow in convergence and require much computing time. In this paper, ant colony optimization is applied to low order harmonic reduction in 7-level, 11-level and 15-level inverters in order to investigate the effect of increasing voltage levels on the feasibility of finding solutions at various values of modulation indices and the harmonic profile of the synthesized output voltage.

II. MULTILEVEL INVERTER

A. Multilevel Inverter Topologies

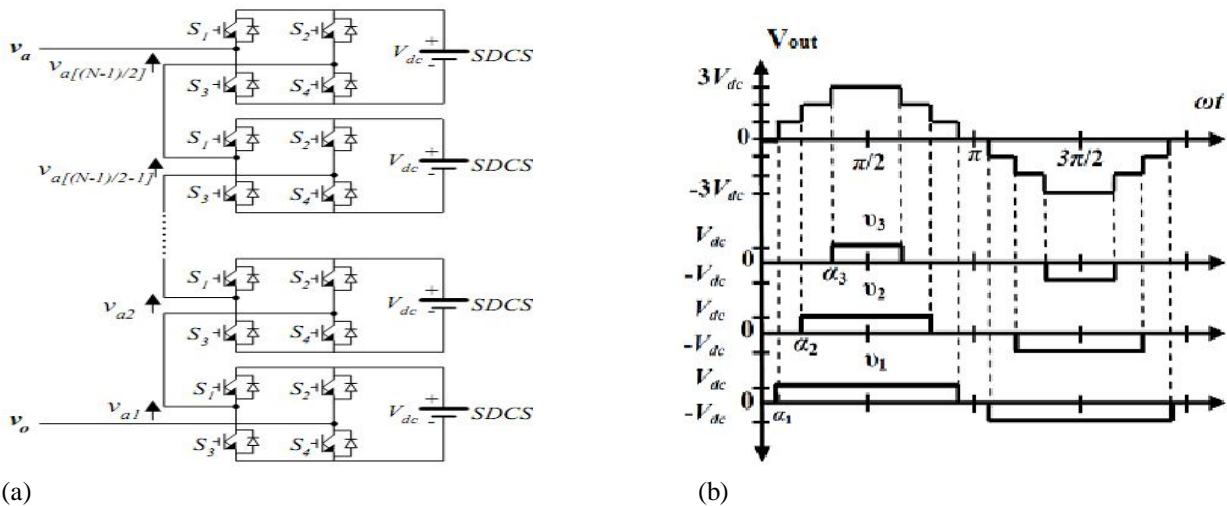
The three main multilevel inverter topologies are diode-clamped inverter which is based on neutral point converter [15], flying capacitor inverter [16], and cascaded H-bridge inverter [17]. With increasing number of levels, flying capacitor inverter becomes more difficult to realize because each capacitor has to be charged with different voltages while diode-clamped inverter suffers from DC link voltage unbalancing problem. Among the topologies, cascaded H-bridge inverter with separate DC sources (SDCS) requires the least number of components. Its modular structure and circuit layout flexibility make it suitable for high voltage and high power applications.

Cascaded H-bridge multilevel inverter is formed by connecting several single-phase H-bridge inverters in series as shown in Figure1 (a) for an N-level inverter. The number of output phase voltage levels in a cascaded H-Bridge inverter is given by $N=2S +1$, where S is the number of cascaded H-bridges per phase. By different combinations of the four switches S_1 , S_2 , S_3 , and S_4 shown in the Figure1 (a), each H-bridge switch can generate a quasi-square wave voltage waveform on the AC side. To obtain $+V_{dc}$, switches S_1 and S_4 are turned on, whereas $-V_{dc}$ can be obtained by turning on switches S_2 and S_3 . By turning on S_1 and S_2 , or S_3 and S_4 , the output voltage is zero. The outputs of H-bridge switches are connected in series such that the synthesized AC voltage waveform is the summation of all voltages from the cascaded H-bridge cells [4], [5].

International Journal of Innovative Research in Science, Engineering and Technology

(An ISO 3297: 2007 Certified Organization)

Vol. 4, Issue 9, September 2015



(a) Single-phase structure of an N-level cascaded multilevel inverter (b) Output voltage waveform of a 7-level inverter.

B. Mathematical Model of SHE-PWM

Generally, any periodic waveform such as the staircase waveform shown in Figure 1(b) can be shown to be the superposition of a fundamental signal and a set of harmonic components. By applying Fourier transformation, these components can be extracted since the frequency of each harmonic component is an integral multiple of its fundamental [18]. With the equal amplitude of all DC sources and quarter wave symmetry, the Fourier series expansion of the staircase output voltage waveform shown in Figure 1 (b) is given by equation (1).

$$v(\omega t) = \sum_{n=1,3,5,\dots}^{\infty} \frac{4V_{dc}}{n\pi} (\cos(n\alpha_1) + \cos(n\alpha_2) + \dots + \cos(n\alpha_s)) \sin n\omega t \quad (1)$$

Subject to $0 < \alpha_1 < \alpha_2 < \dots < \alpha_s \leq \pi/2$

Where S is the number of switching angles and n is the harmonic order. For 7-level, 11-level and 15-level inverters, the numbers of SDCSs required are three, five, and seven, respectively. In three-phase power system, the triplen harmonics in each phase need not be cancelled as they automatically cancel in the line-to-line voltages as a result only non-triplen odd harmonics are present in the line-to-line voltages [8]. Generally, for S number of switching angles, one switching angle is used for the desired fundamental output voltage V_1 and the remaining $(S-1)$ switching angles are used to eliminate certain low order harmonics that dominate the total harmonic distortion (THD) such that equation (1) becomes

$$V(\omega t) = V_1 \sin(\omega t) \quad (2)$$

From equation (1), the expression for the fundamental output voltage V_1 in terms of the switching angles is given by

$$V_1 = \frac{4V_{dc}}{\pi} (\cos(\alpha_1) + \cos(\alpha_2) + \dots + \cos(\alpha_s)) \quad (3)$$

The relation between the fundamental voltage and the maximum obtainable fundamental voltage V_{1max} is given by modulation index. The modulation index, m_i , is defined as the ratio of the fundamental output voltage V_1 to the maximum obtainable fundamental voltage V_{1max} . The maximum fundamental voltage is obtained when all the switching angles are zero [4]. From equation (3),

$$V_{1max} = \frac{4sV_{dc}}{\pi} \quad (4)$$

$$\therefore m_i = \frac{V_1}{V_{1max}} = \frac{\pi V_1}{4sV_{dc}} \text{ such that } V_1 = m_i \left(\frac{4sV_{dc}}{\pi} \right) \text{ for } 0 < m_i \leq 1 \quad (5)$$

International Journal of Innovative Research in Science, Engineering and Technology

(An ISO 3297: 2007 Certified Organization)

Vol. 4, Issue 9, September 2015

The modulation index and switching angles that result into the synthesis of AC waveform with the least Total Harmonic Distortion (THD) can be found by solving S number of transcendental nonlinear equations known as SHE equations that characterize the selected harmonics[4], [5]. For 7-level inverter, SHE equations are as follows:

$$\begin{aligned} \cos(\alpha_1) + \cos(\alpha_2) + \cos(\alpha_3) &= 3m_i \\ \cos(5\alpha_1) + \cos(5\alpha_2) + \cos(5\alpha_3) &= 0 \\ \cos(7\alpha_1) + \cos(7\alpha_2) + \cos(7\alpha_3) &= 0 \end{aligned} \quad (6)$$

$$\text{Subject to } 0 \leq \alpha_1 < \alpha_2 < \alpha_3 \leq \frac{\pi}{2} \quad (7)$$

Similarly, for an 11-level inverter:

$$\begin{aligned} \cos(\alpha_1) + \cos(\alpha_2) + \cos(\alpha_3) + \cos(\alpha_4) + \cos(\alpha_5) &= 5m_i \\ \cos(5\alpha_1) + \cos(5\alpha_2) + \cos(5\alpha_3) + \cos(5\alpha_4) + \cos(5\alpha_5) &= 0 \\ \cos(7\alpha_1) + \cos(7\alpha_2) + \cos(7\alpha_3) + \cos(7\alpha_4) + \cos(7\alpha_5) &= 0 \\ \cos(11\alpha_1) + \cos(11\alpha_2) + \cos(11\alpha_3) + \cos(11\alpha_4) + \cos(11\alpha_5) &= 0 \\ \cos(13\alpha_1) + \cos(13\alpha_2) + \cos(13\alpha_3) + \cos(13\alpha_4) + \cos(13\alpha_5) &= 0 \end{aligned} \quad (8)$$

$$\text{Subject to } 0 \leq \alpha_1 < \alpha_2 < \alpha_3 < \alpha_4 < \alpha_5 \leq \frac{\pi}{2} \quad (9)$$

Lastly, for a 15-level inverter,

$$\begin{aligned} \cos(\alpha_1) + \cos(\alpha_2) + \cos(\alpha_3) + \cos(\alpha_4) + \cos(\alpha_5) + \cos(\alpha_6) + \cos(\alpha_7) &= 7m_i \\ \cos(5\alpha_1) + \cos(5\alpha_2) + \cos(5\alpha_3) + \cos(5\alpha_4) + \cos(5\alpha_5) + \cos(5\alpha_6) + \cos(5\alpha_7) &= 0 \\ \cos(7\alpha_1) + \cos(7\alpha_2) + \cos(7\alpha_3) + \cos(7\alpha_4) + \cos(7\alpha_5) + \cos(7\alpha_6) + \cos(7\alpha_7) &= 0 \\ \cos(11\alpha_1) + \cos(11\alpha_2) + \cos(11\alpha_3) + \cos(11\alpha_4) + \cos(11\alpha_5) + \cos(11\alpha_6) + \cos(11\alpha_7) &= 0 \\ \cos(13\alpha_1) + \cos(13\alpha_2) + \cos(13\alpha_3) + \cos(13\alpha_4) + \cos(13\alpha_5) + \cos(13\alpha_6) + \cos(13\alpha_7) &= 0 \\ \cos(17\alpha_1) + \cos(17\alpha_2) + \cos(17\alpha_3) + \cos(17\alpha_4) + \cos(17\alpha_5) + \cos(17\alpha_6) + \cos(17\alpha_7) &= 0 \\ \cos(19\alpha_1) + \cos(19\alpha_2) + \cos(19\alpha_3) + \cos(19\alpha_4) + \cos(19\alpha_5) + \cos(19\alpha_6) + \cos(19\alpha_7) &= 0 \end{aligned} \quad (10)$$

$$\text{The correct solution must satisfy the condition } 0 \leq \alpha_1 < \alpha_2 < \dots < \alpha_7 \leq \frac{\pi}{2} \quad (11)$$

Generally equations (6), (8), and (10) can be written as

$$F(\alpha) = B(m_i) \quad (12)$$

For each multilevel inverter structure, total harmonic distortion (THD) is computed as shown in equation (13):

$$THD = \sqrt{\sum_{i=5,7,11,13,\dots}^{49} \left(\frac{V_i}{V_1}\right)^2} \quad (13)$$

III. ANT COLONY OPTIMIZATION (ACO)

The ant colony optimization is swarm intelligence based meta-heuristic algorithm that was inspired by the food foraging behavior of natural ants. It is a probabilistic technique for solving combinatorial optimization problems that can be reduced to finding good path through graphs. In their search for food, natural ants leave a trail of chemical substance called pheromone on the path they traverse in order to guide future ants toward optimal paths to food. The pheromone on the non-optimal paths evaporates with time while the pheromone on the near-optimal/optimal paths is reinforced, thus influencing more ants to follow the path [19]. In ACO, a population of agents (artificial ants) incrementally constructs solutions to combinatorial optimization problem by traversing a graph that encodes the optimization problem. Ant Colony system (ACS) algorithm, introduced by Dorigo and Gambardella [20] has been successfully deployed for discrete combinatorial optimization problems such as routing, and clustering. ACO algorithm has been extended to solving continuous combinatorial optimization problems using a variety of ACO algorithm called Variable Sampling Ant Colony Optimization (SamACO) algorithm [21]. SamACO algorithm offers an efficient incremental solution construction method based on the sampled values. The basic idea behind SamACO algorithm is that a population of agents (artificial ants) incrementally constructs solution to the sampled combinatorial optimization problem. The construction phase is guided by heuristic information and existing pheromone, which hold information

International Journal of Innovative Research in Science, Engineering and Technology

(An ISO 3297: 2007 Certified Organization)

Vol. 4, Issue 9, September 2015

about parts of a solution that have led to good results in the previous generation of ants. By means of pheromone update and transition rules, ACO probabilistically select the components values to concentrate the search in the regions of high quality solutions.

The steps that are involved in the implementation of SamACO algorithm are as follows:

Initialization step: The search space is bounded such that the decision variables (solution components) X_i has values $x_i \in [l_i, u_i]$, $i = 1, 2, \dots, S$ where l_i and u_i are the lower and upper bounds of the decision variables X_i , respectively, and S is the number of decision variables. The initial values of the decision variables are randomly sampled in the feasible domain as follows:

$$x_i^{(j)} = l_i + \frac{u_i - l_i}{P} (j - 1 + \text{rand}^{(j)}) \quad (14)$$

Where P is the population size divided into two pools such that $P = m + \theta$, m is the number of ants, θ is the exploitation frequency which controls the number of values to be sampled in the neighborhood of the best-so-far solution per iteration, and rand is a random number uniformly distributed within $[0, 1]$, $i = 1, 2, \dots, S$ and $j = 1, 2, \dots, (m + \theta)$. For each decision variable X_i , there are k_i sampled values $x_i^{(1)}, x_i^{(2)}, \dots, x_i^{(k_i)}$ from the continuous domain $[l_i, u_i]$. Each solution component has associated a pheromone value, τ_i^j , $i = 1, 2, \dots, S$, $j = 1, 2, \dots, k_i$, and a component-pheromone matrix M can be generated. The pheromone value τ_i^j reflects the desirability of adding the component value x_i^j to the solution

$$M = \begin{bmatrix} \{x_1^{(1)}, \tau_1^{(1)}\} & \{x_2^{(1)}, \tau_2^{(1)}\} & \dots & \{x_s^{(1)}, \tau_s^{(1)}\} \\ \{x_1^{(2)}, \tau_1^{(2)}\} & \{x_2^{(2)}, \tau_2^{(2)}\} & \dots & \{x_s^{(2)}, \tau_s^{(2)}\} \\ \vdots & \vdots & \ddots & \vdots \\ \{x_1^{(k_i)}, \tau_1^{(k_i)}\} & \{x_2^{(k_i)}, \tau_2^{(k_i)}\} & \dots & \{x_s^{(k_i)}, \tau_s^{(k_i)}\} \end{bmatrix} \quad (15)$$

Transition: The transition of the ants from one position to another is partially probabilistic and partially deterministic. An artificial ant k has a memory of the positions that it has already visited and the pheromone content at each location stored in a Tabu list T^k . The memory size of the Tabu list depends on the ant population size as well as the number of movement made by the ants. In general, if there are m ants making N movement, the size of the Tabu list is $(m \times N)$. The iteration index l_i^k of the variable value selected by ant k for the i^{th} variable is:

$$l_i^k = \begin{cases} 1 & \text{if } q \leq q_o \text{ and } j = j^* \\ 0 & \text{if } q \leq q_o \text{ and } j \neq j^* \\ L_i^{(k)} & \text{if } q > q_o \end{cases} \quad \text{Where } j^* = \arg \max \{ \tau_i^{(1)}, \tau_i^{(2)}, \dots, \tau_i^{(m)} \} \quad (16)$$

$i = 1, 2, \dots, s$, $k = 1, 2, \dots, m$, $q \in [0, 1]$ is a uniform random value, and $q_o \in [0, 1]$ is a threshold parameter that represents the relative preference for either exploitation or exploration.

Dynamic exploitation: When $q \leq q_o$, the ant chooses exploitation in the neighborhood of the solution set with the highest pheromone value from the m solutions generated in the previous iteration. The dynamic exploitation is used as a local search method to fine-tune the best-so-far solution. A radius r_i confines the search in the neighborhood of the best-so-far solution $x^{(0)} = (x_1^{(0)}, x_2^{(0)}, \dots, x_s^{(0)})$ to the interval $[x_i^{(0)} - r_i, x_i^{(0)} + r_i]$, $i = 1, 2, \dots, S$. The values of the variables in the best-so-far solution set are randomly selected to be increased, unchanged or reduced as

$$\hat{x}_i = \begin{cases} \min(x_i^{(0)} + r_i \cdot \sigma_i, u_i), & 0 \leq q < \frac{1}{3} \\ x_i^{(0)}, & \frac{1}{3} \leq q < \frac{2}{3} \\ \max(x_i^{(0)} - r_i \cdot \sigma_i, l_i), & \frac{2}{3} \leq q < 1 \end{cases} \quad \text{Where } \sigma \in [0, 1] \quad (17)$$

International Journal of Innovative Research in Science, Engineering and Technology

(An ISO 3297: 2007 Certified Organization)

Vol. 4, Issue 9, September 2015

The best-so-far solution set is then updated using elitism and generational replacement. The new solution set $\hat{x} = (\hat{x}_1, \hat{x}_2, \dots, \hat{x}_S)$ is evaluated and used to replace the best-so-far solution set if there is an improvement in the result. The dynamic exploitation process is repeated for g times, and the newly generated solution components are recorded as $x_i^{(j)}$, where $j = m+1, m+2, \dots, m+g_i, i = 1, 2, \dots, S$. The number of solution components generated during the dynamic exploitation process is denoted by g_i . The radii are adaptively extended or reduced based on the exploitation result. If the best solution set produced by the exploitation process is better than the prevailing best-so-far solution set, the radii will be extended. Otherwise, the radii will be reduced.

$$r_i \leftarrow \begin{cases} r_i \cdot v_e, & v_e > 1 \\ r_i \cdot v_r, & 0 < v_r \leq 1 \end{cases} \quad (18)$$

Where v_e and v_r are the radius extension rate and the radius reduction rate, respectively. The initial radius value is given by:

$$r_i = \frac{u_i - l_i}{2m} \quad (19)$$

Random exploration: when $q > q_o$, the ant resort to probabilistic exploration to select a random index $L_i^{(k)} \in \{0, 1, \dots, m+g_i\}$. Moving from position i , the ant chooses its next position j among the positions that have not been visited yet according to the probability distribution given as follows:

$$p_i^{(j)} = \frac{\tau_i^{(j)}}{\sum_{u=0}^{m+g_i} \tau_i^{(u)}}, \quad j = 0, 1, \dots, m+g_i \quad (20)$$

The solution components of the worst x solution sets that are constructed by the ants in the previous iteration are discarded and each solution component is replaced by x new values generated by a random exploration process. If the worst solution sets are denoted by $x^{(m-x+1)}, x^{(m-x+2)}, \dots, x^{(m)}$. The new solution components for the solution set $x^{(j)}$ are randomly generated as follows:

$$x^{(j)} = l_i + (u_i - l_i) \cdot \text{rand}_i^{(j)} \quad \text{Where } i = 1, 2, \dots, S \text{ and } j = (m-x+1), (m-x+2), \dots, m \quad (21)$$

Random exploration ensures diversity and prevents premature convergence to local minima.

Pheromone update: Initially, each solution component is assigned an initial pheromone value τ_o . The pheromone values are updated based on the quality of solutions constructed by the ants. The update is biased towards the best solutions constructed by the ants such that ACO concentrates the search in the regions of high quality solutions. Similar to MAX-MIN ant system [22], the pheromone values in SamACO algorithm are bounded to the interval $[T_{\min}, T_{\max}]$; in this case $[0.1, 1]$. The pheromones on the non-optimal paths are evaporated. The selected non-optimal solution components have their pheromones evaporated as

$$\tau_i^{(j)} \leftarrow (1-\rho)\tau_i^{(j)} + \rho\tau_{\min} \quad \text{for } 0 < \rho < 1 \quad (22)$$

Where τ_{\min} is the predefined minimum pheromone value, ρ is the pheromone evaporation rate, $i = 1, 2, \dots, S$ and $j = 1, 2, \dots, m$.

The pheromones on the near optimal paths are reinforced, thus influencing more ants to follow the paths and hopefully find better solutions. The solution components in the selected best Ψ solutions have their pheromone reinforced as

$$\tau_i^{(j)} \leftarrow (1-\beta)\tau_i^{(j)} + \beta\tau_{\max} \quad \text{for } 0 < \beta < 1 \quad (23)$$

Where τ_{\max} is the predefined maximum pheromone value, β is the pheromone reinforcement rate, Ψ is the elitist number, $i = 1, 2, \dots, S$ and $j = 1, 2, \dots, \Psi$. In each iteration, the pheromone values of the solution components of the iteration-best are updated as the solution components of the best-so-far solution after the fitness evaluation of the m solutions constructed by the ants.

International Journal of Innovative Research in Science, Engineering and Technology

(An ISO 3297: 2007 Certified Organization)

Vol. 4, Issue 9, September 2015

IV. IMPLEMENTATION

Using MATLAB software, the proposed SamACO algorithm was implemented to solve SHE equations (6), (8), and (10) that characterize the selected harmonics in 7-, 11-, and 15-level inverter, respectively. In the three cases, the population size is 40, and the number of iterations is 100. The solutions were computed by incrementing the modulation index, m_i in steps of 0.001 from 0 to 1. A personal computer (2.66 GHz Intel Corei7 processor with 4GB Random Access Memory) running MATLAB R2014b on OS X Yosemite version 10.10 was used to carry out the computations.

The solution set at each step is evaluated with the fitness function. The objective here is to determine the switching angles such that the selected low order harmonics are either eliminated or minimized to an acceptable level while the fundamental voltage is obtained at a desired value. For each solution set, the fitness function is calculated as follows [14]:

$$f = \min_{\alpha_i} \left[\left(100 \frac{V_i^* - V_1}{V_1^*} \right)^4 + \sum_{s=2}^S \frac{1}{h_s} \left(50 \frac{V_{hs}}{V_1} \right)^2 \right] \text{ where } i = 1, 2, \dots, S \quad (24)$$

Subject to equas. (7), (9), and (11) for 7-level, 11-level, and 15-level CMLI, respectively. For values of the fitness function less or equal to 0.01, SHE equations are solvable without constraint violation, otherwise they are unsolvable.

In order to validate the observed analytical results, the three multilevel inverter structures, namely: 7-level, 11-level and 15-level single-phase Cascaded H-Bridge inverters were modelled in MATLAB-SIMULINK using SimPower System block set. In each of H-Bridges in the inverters, 12V dc source is the SDCS, and the switching device used is Insulated Gate Bipolar Transistor (IGBT). Simulations were performed at the fundamental frequency of 50 Hz using the solution set of each inverter structure at the same arbitrarily chosen modulation index of 0.819.

V. RESULTS

A. Results for the Seven-Level Inverter

In case of 7-level CMLI, there are three switching angles such that there are three switching instants per quarter cycle. Shown in Figure 2 (a) is the plot of fitness function for each set of switching angles versus modulation indices over the range of 0.1 to 1.0.

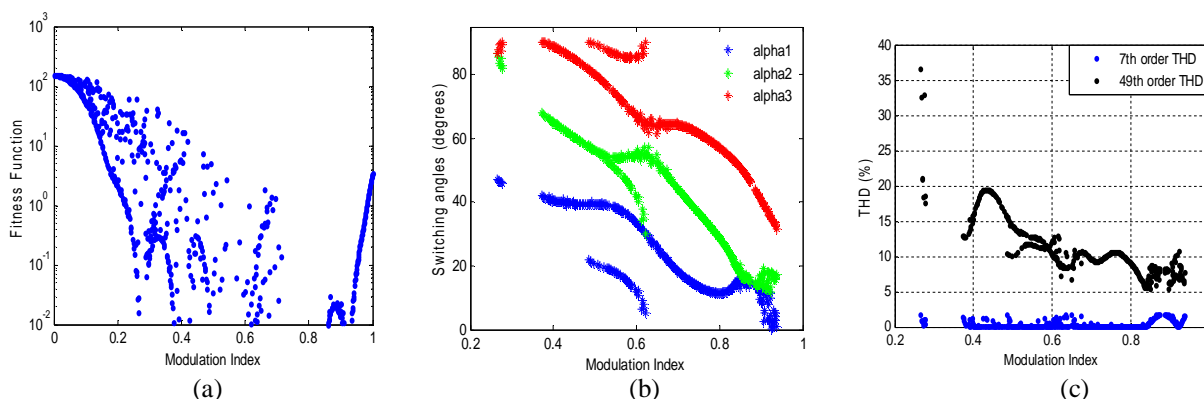


Figure 2: Plots of (a) Fitness function (b) Switching angles (c) THD versus modulation index for 7-level CMLI.

Figure 2 (b) shows the plot of switching angles that eliminate 3rd and 5th harmonics for different values of modulation index. It is observed that there are no solutions in the lower interval [0, 0.263] and upper interval [0.938, 1]. As shown in Figure 2(b), there are multiple solution sets at some modulation indices, while none exist in some intervals. In event of multiple solution sets, the solution set with the least THD value is chosen. The 7th order THD and 49th order THD curves for the corresponding solution sets of 7-level inverter are shown in Figure 2 (c). It is apparent that 49th order THD is more than 5% for all values of modulation index. This shows that none of the solution sets meets IEEE-519 standard.

International Journal of Innovative Research in Science, Engineering and Technology

(An ISO 3297: 2007 Certified Organization)

Vol. 4, Issue 9, September 2015

Presented in Table I are some values of switching angles that eliminate 3rd and 5th harmonics in a 7-level inverter at different modulation indices.

TABLE I
Some values of switching angles (in degrees) for 7-level CMLI

m_i	Switching Angles		
	α_1	α_2	α_3
0.489	21.3956	57.4530	90
0.681	20.7605	47.1337	64.6675
0.795	11.5256	29.5773	57.6188
0.819	12.0573	25.1332	54.9791
0.925	1.7709	17.7541	34.8341

B. Results for the Eleven-Level Inverter

SHE equations (8) are solved to compute the five switching angles that eliminate 5th, 7th, 11th and 13th harmonics. Shown in Figure 3 (a) is the plot of fitness function of solution sets at different modulation indices within the range of 0 to 1. The summary of the switching angles obtained are shown in Figure 3 (b). Apparently, there are no solutions in the lower interval [0, 0.255] and upper interval [0.935, 1]. The plots of the corresponding 13th order THD and 49th order THD versus modulation index are shown in Figure 3 (c) for each of the solution sets in Figure 3 (b).

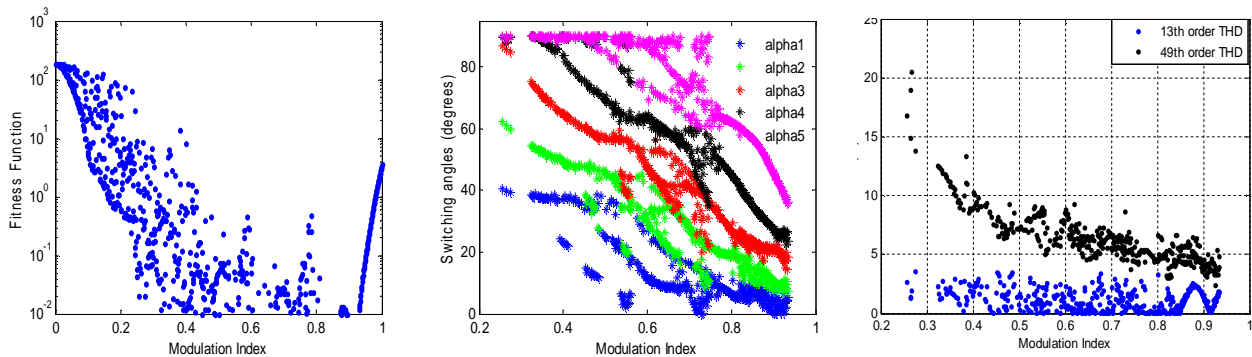


Figure 3: Plots of (a) Fitness function (b) Switching angles (c) THD versus modulation index for 11-level CMLI. Some values of switching angles that eliminate 3rd, 5th, 7th, and 13th harmonics in 11-level inverter at different modulation indices are presented in Table II.

TABLE II
Some values of switching angles (in degrees) for 11-level CMLI

m_i	Switching Angles				
	α_1	α_2	α_3	α_4	α_5
0.489	38.0674	44.1473	57.9826	70.9300	85.1275
0.681	17.0238	30.2759	48.5112	58.1070	66.6863
0.795	6.9903	19.0532	28.0094	45.9851	62.6068
0.819	5.0277	18.7928	24.0067	41.7131	60.5656
0.925	3.8366	9.5008	16.5330	26.9495	38.2513

C. Results for the Fifteen-Level Inverter

Similarly, solutions of equation (13) are computed based on the fitness evaluation shown in Figure 4 (a). The feasible solutions are plotted in Figure 4 (b) against the modulation index. As shown in the figure, there are no solutions in the lower interval [0, 0.435] and upper interval [0.933, 1]. The corresponding 19th order THD and 49th order THD are plotted for each solution set as shown in Figure 4 (c).

International Journal of Innovative Research in Science, Engineering and Technology

(An ISO 3297: 2007 Certified Organization)

Vol. 4, Issue 9, September 2015

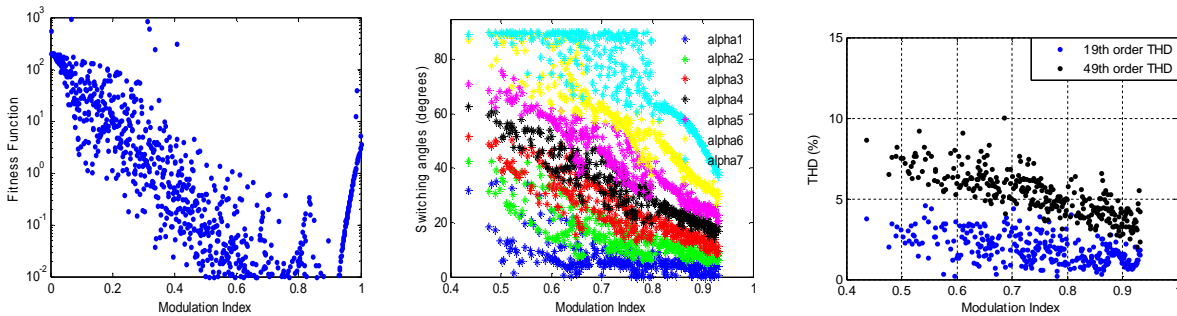


Figure 4: Plots of (a) Fitness function (b) Switching angles (c) THD versus modulation index for 15-level CMLI

It is observed from Figures 2 (b), 3 (b) and 4 (b) that multiple solution sets exist at some modulation indices. In such cases, THD is computed for each of the multiple solution sets and the set with the least THD value is chosen and termed as combined solution. It can be seen in Figures 2 (c), 3 (c) and 4 (c) that THD values are very high at the lower end of modulation indices and they are considerably reduced at the upper end.

Some values of switching angles that attenuate 3rd, 5th, 7th, 13th, 17th and 19th harmonics in 15-level inverter at different modulation indices are presented in Table III.

TABLE III
Some values of switching angles (in degrees) for 15-level CMLI

m_i	Switching Angles						
	α_1	α_2	α_3	α_4	α_5	α_6	α_7
0.489	17.19	30.55	49.88	60.76	62.38	89.71	90.00
0.681	11.95	24.10	35.33	46.68	54.20	62.99	71.59
0.795	5.00	13.25	21.38	29.47	39.92	53.84	63.88
0.819	4.12	11.94	19.90	25.90	39.12	48.25	62.34
0.925	2.93	6.94	10.98	17.33	23.70	30.51	40.37

Comparative analysis of the results obtained for the three multilevel inverter structures shows that 7-level and 11-level inverters are at par in terms of range of modulation indices for which solutions of SHE equations (6) and (8) exist, while 15-level has a narrow range. With increasing number of levels, complexities and cases of multiple solution sets increase as well. Both 11-level and 15-level inverters have lower THD compared with 7-level inverter for all values of modulation indices. However, 11-level inverter has lower THD compared with 15-level inverter at some modulation indices.

Fast Fourier Transform analyses of the simulated phase voltage waveforms were done using the FFT block to show the harmonic spectrum of the synthesized AC voltages. The following are observed from the FFT plots (Figures 5, 6 and 7): (i) in 7-level inverter, 5th and 7th harmonics are considerably eliminated as their values tend towards zero. 7th order THD of the inverter is 0.2%. (ii) Similarly, in 11-level inverter 5th, 7th, 11th and 13th harmonics are well attenuated as their values tend towards zero, and 13th order THD is 0.1% (iii) 5th, 7th, 11th, 13th, 17th, and 19th harmonics are only minimized in 15-level inverter, as they still constitute a significant part of the THD. 19th order THD of the inverter is 2.44%. The results of the performance evaluation of the multilevel inverter structures in terms of the selected low order harmonics elimination are presented in Table IV.

International Journal of Innovative Research in Science, Engineering and Technology

(An ISO 3297: 2007 Certified Organization)

Vol. 4, Issue 9, September 2015

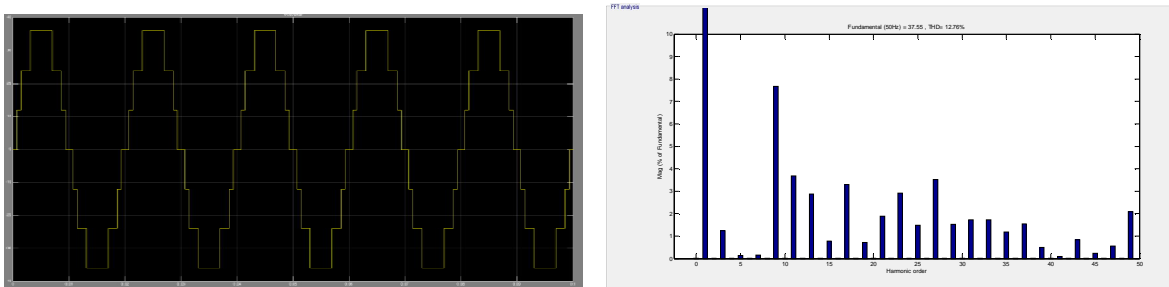


Figure 5: Phase output voltage waveform of 7-level inverter and its FFT plot

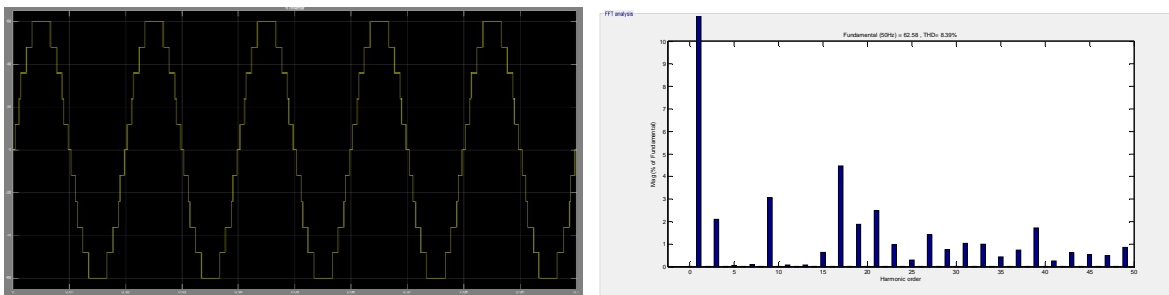


Figure 6: Phase output voltage waveform of 11-level inverter and its FFT plot

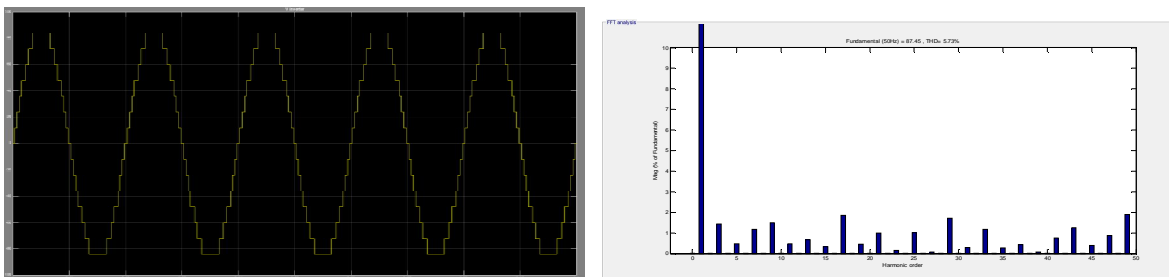


Figure 7: Phase output voltage waveform of 15-level inverter and its FFT plot.

TABLE IV
Harmonic profiles of the three multilevel Inverter structures.

Order of THD	THD (%)		
	7-level inverter	11-level inverter	15-level inverter
7 th	0.2	0.1	1.27
13 th	4.67	0.14	1.52
19 th	5.76	4.84	2.44
49 th	7.63	5.32	4.09

The THD in line-to-line voltages of the three multilevel inverter structures as computed analytically and from simulations are presented in Table V. The analytical and simulation values of THD are in close agreement thereby validating the analytical results. The THD values of 12.76%, 8.39% and 5.73% shown in Figure 5, 6, and 7, respectively

International Journal of Innovative Research in Science, Engineering and Technology

(An ISO 3297: 2007 Certified Organization)

Vol. 4, Issue 9, September 2015

are the THD values of the synthesized phase voltages which includes triplen harmonic components. The line-to-line harmonic content of a three phase system is the same as a single phase system, less the triplen harmonics.

TABLE V
Line-to-line THD values of the three multilevel inverter structures.

Inverter Structure	Line voltage THD (%)	
	Analytical Value	Simulation Value
7-level inverter	7.47	7.63
11-level inverter	5.34	5.32
15-level inverter	4.15	4.09

Presented in Table VI are the values of fundamental voltage for the three multilevel inverter structures as analytically computed with equation (13), and by simulations.

Table VI
Values of fundamental voltage for the three multilevel inverter structures

Inverter Structure	Fundamental Voltage (V)	
	Analytical Value	Simulation Value
7-level inverter	37.54	37.55
11-level inverter	62.57	62.58
15-level inverter	87.59	87.45

It can be seen from Table VI that analytically computed values of fundamental voltages closely agree with the simulation values.

VI. CONCLUSION

Variable Sampling Ant Colony optimization (SamACO) algorithm with random initial values has been successfully implemented for solving SHE equations that characterize harmonics in 7-, 11-, and 15-level inverters. Analytical results are validated with simulations results in all cases. The performance of the three multilevel inverter structures in terms of fundamental voltage, THD contents, capability for selected harmonic elimination, and complexities has been investigated. It has been observed that while output voltage increases with increasing number of levels, cost and complexity in computation of solution sets increase as well. Among the three multilevel inverters, 11-level inverter is the only inverter structure that is able to meet wide modulation range and high power quality requirements of applications such as drives.

REFERENCES

- [1] R. H. Baker and L. H. Bannister, "Electric power converter," U.S. Patent 3867643, Feb. 1975.
- [2] K. A. Corzine, "Multi-Level Converters," The Handbook on Power Electronics, Edited by T.L. Skvarenina, CRC Press, 2002, pp. 6-1 - 6-23
- [3] J. Rodríguez, J. Lai, F.Peng, "Multilevel inverters: a survey of topologies, controls and applications," *IEEE Transactions on Industry Applications*, vol. 49, no. 4, Aug. 2002, pp. 724-738.
- [4] J. Kumar, B. Das, and P. Agarwal, "Selective Harmonic Elimination Technique for Multilevel Inverter," 15th National Power System Conference (NPSC), IIT Bombay, 2008, pp. 608-613.
- [5] J. N. Chiasson, L. M. Tolbert, K. J. McKenzie, and Z. Du, "Control of a Multilevel Converter Using Resultant Theory," *IEEE Transaction on Control Systems Technology*, volume 11, no. 3, May 2003, pp. 345- 353.
- [6] F. Swift and A. Kamberis, "A New Walsh Domain Technique of Harmonic Elimination and Voltage Control In Pulse-Width Modulated Inverters," *IEEE Transactions on Power Electronics*, volume 8, no. 2, 1993, pp. 170-185.
- [7] T. J. Liang and R. G. Hoft, "Walsh Function Method of Harmonic Elimination," *Proceedings of IEEE Appl. Power Electron. Conference*, 1993, pp.847-853.

International Journal of Innovative Research in Science, Engineering and Technology

(An ISO 3297: 2007 Certified Organization)

Vol. 4, Issue 9, September 2015

- [8] T. J. Liang, R. M. O'Connell, R. M. and R. G. Hoft, "Inverter Harmonic Reduction Using Walsh Function Harmonic Elimination Method," IEEE Transaction on Power Electron, volume 12, no. 6, 1997, pp. 971-982.
- [9] B. Ozpineci, L. M. Tolbert, and J. N. Chiasson, "Harmonic Optimization of Multilevel Converters using Genetic Algorithm," 35 Annual IEEE Power Electronics Specialists Conference, Germany, 2004.
- [10] R. Salehi, N. Farokhia, M. Abedi, and S.H. Fathi, "Elimination of Low Order Harmonics in Multilevel Inverters Using Genetic Algorithm," Journal of Power Electronics, volume 11, no. 2, Mar. 2011, pp. 132-139.
- [11] D.O. Aborisade, I.A. Adeyemo, and C.A. Oyeleye, "Harmonic Optimization in Multilevel Inverter Using Real Coded Genetic Algorithm," International Journal of Electrical Engineering Research & Applications (IJEERA) volume 1, Issue 4, 2013.
- [12] N. Vinoth, and H. Umeshprabhu, "Simulation of Particle Swarm Optimization Based Selective Harmonic Elimination," International Journal of Engineering and Innovative Technology (IJEIT) Volume 2, Issue 7, 2013, pp. 215-218.
- [13] K. Sundareswaran, K. Jayant, and T. N. Shanavas, "Inverter Harmonic Elimination through a Colony of Continuously Exploring Ants," IEEE Transactions on Industrial Electronics, volume 54, no. 5, 2007, pp. 2558-2565.
- [14] A. Kavousi, et. al., "Application of the Bee Algorithm for Selective Harmonic Elimination Strategy in Multilevel Inverters," IEEE Transaction on Power Electronics, vol. 27, no. 4, pp. 1689-1696, April 2012.
- [15] A. Nabae, I. Takahashi and H. Akagi, "A new neutral-point clamped PWM inverter," IEEE Trans. Ind. Applicat., vol. IA-17, Sept./Oct. 1981, pp. 518-523.
- [16] T. A. Meynard and H. Foch, "Multi-level conversion: High voltage choppers and voltage- source inverters," in Proc. IEEE-PESC, 1992, pp. 397-403.
- [17] P. Hammond, "A new approach to enhance power quality for medium voltage ac drives," IEEE Trans. Ind. Applicat., vol. 33, Jan./Feb. 1997, pp. 202-208
- [18] S. Sirisukprasert, J. S. Lai, and T. H. Liu, "Optimum Harmonic with a Wide Range of Modulation Indices for Multilevel Converters," IEEE Transaction on Industrial Electronics, Vol. 49, no; 4, August 2002, pp. 875-881.
- [19] M. Dorigo, V. Maniezzo, and, A. Colomi, "Ant System: Optimisation by a colony of Cooperating Agents." IEEE Transactions on Systems, Man, and Cybernetics, Part B, volume 26, no. 1, 1996, pp. 29-41.
- [20] M. Dorigo and L. Gambardella, "Ant Colony System: A cooperative Learning Approach to the Travelling Salesman Problem," IEEE Transactions on Evolutionary Computation, volume 1, no. 1, 1997, pp. 53-66.
- [21] X. Hu, J. Zhang, H. S. Chung, Y. Li, and O. Liu, "SamACO: Variable Sampling Ant Colony Optimisation for Continuous Optimisation," IEEE Transactions on Systems, Man, and Cybernetics, 40 (6), 2010, pp 1-36.
- [22] T. Stützle and H. H. Hoos, "MAX-MIN Ant System," Future Generation Computer Systems, volume 16, no. 8, 2000, pp. 889-914